Journal of Advanced Ceramics
2015, **4**(4): 318–325
DOI: 10.1007/s40145-015-0168-7

ISSN 2226-4108
CN 10-1154/TQ

Research Article

Luminescence enhancement of $CaMoO_4:Eu^{3+}$ phosphor by charge compensation using microwave sintering method

Zhiping ZHOU, Yingsen YU, Xiaotang LIU*, Weihao YE, Guangqi HU, Bingfu LEI, Yun YAN

College of Materials and Energy, South China Agricultural University, Guangzhou 510642, China

Received: May 27, 2015; Revised: August 09, 2015; Accepted: August 25, 2015

Abstract: $CaMoO_4:Eu^{3+}$ and $CaMoO_4:Eu^{3+},A^+$ (A = Li, Na, K) phosphors for light-emitting diode (LED) applications have been prepared by microwave sintering method (MSM), and their structure and luminescence properties are investigated. The influences of microwave reaction time and concentration of different kinds of charge compensation A^+ and Eu^{3+} on luminescence have also been discussed. The samples emit a red luminescence at 615 nm attributed to the $^5D_0 \rightarrow {}^7F_2$ transition of Eu^{3+} under 464 nm excitation. It is observed that adding charge compensation A^+ in the sample synthesis increases luminescence intensity. The optimized sample made with 32 mol% Li^+ and 32 mol% Eu^{3+} has an enhancement factor of 4 in photoluminescence compared to the sample made without charge compensation. The CIE (Commission Internationale de l´Eclairage) coordinates of $Ca_{0.36}MoO_4:0.32Eu^{3+},0.32Li^+$ are $x = 0.661$ and $y = 0.339$, which indicate that the obtained phosphor can be a promising red color candidate for white LED fabrications.

Keywords: $CaMoO_4:Eu^{3+}$ phosphor; luminescence enhancement; charge compensation; microwave sintering; white light-emitting diode (LED)

1 Introduction

After the first commercial light-emitting diode (LED) based on GaN blue-emitting chip and Ce^{3+} activated yttrium aluminum garnet ($YAG:Ce^{3+}$) yellow phosphor was fabricated in 1997 [1], white LEDs [2,3] have brought a new surge of revolution in illumination by replacing traditional incandescent or fluorescence lamps. With their advantages of high efficiency, long lifetime, and non-pollution, LEDs have been widely applied in lighting and display devices, including plasma display panel, field emission display, white light diode, etc. [4–7]. However, white LEDs with GaN based blue-emitting chips and yellow–red phosphors have poor color rendering index due to the deficiencies in red emission [8] in current market. In order to solve this problem, two ways are usually recommended for phosphor converted LEDs. The first one is to add red-emitting phosphor in the white LEDs based on blue-emitting chips and yellow phosphor system. The other is to adopt ultraviolet (UV) or near-UV LED chips and tricolor (red, green, and blue) phosphor system. The current commercial tricolor phosphors are mainly $Y_2O_2S:Eu^{3+}$ for red, $ZnS:Cu^+,Al^{3+}$ for green, and $BaMgAl_{10}O_{17}:Eu^{2+}$ for blue [9,10]. Nonetheless, the poor stability of $Y_2O_2S:Eu^{3+}$ makes it less desirable due to the release of sulfide gas, lower efficiency, and shorter working lifetime under UV irradiation than the green and blue

* Corresponding author.
E-mail: xtliu@scau.edu.cn

phosphors [11]. Therefore, to exploit efficient red phosphors with high luminance, suitable chromaticity coordinates, and good stability in the near-UV region is an urgent and challenging research task.

Nowadays, some red phosphors, such as molybdates [12], tungstates [13], aluminates [14], and nitride phosphors [15], are attracting more and more attention as they are able to overcome the drawback of poor color rendering index of cool white LEDs. It has been reported that Eu^{3+} activated $CaMoO_4$ phosphor has higher efficient emission intensity under near-UV excitation, more satisfactory chromaticity coordinates, and better stability than sulfide phosphors [16]. However, its red emission intensity still needs to be improved. Compared to conventional research methods, such as the high temperature solid state reaction (SSR) and co-precipitation method, by which it may need several hours of calcination at 800–1100 ℃, microwave sintering is featured with faster heating up (about 30 min using a microwave oven of 800 W) and has higher efficiency, better uniformity of sintering temperature, and an obvious effect of energy saving.

In this work, the effect of different charge compensations on the luminescence property of Eu^{3+} doped $CaMoO_4$ has been investigated by the microwave sintering method (MSM). The result shows that charge compensations can significantly improve the emission intensity of Eu^{3+} doped $CaMoO_4$, and the developed phosphor is expected to exhibit superior spectroscopic properties as a single-component UV-convertible phosphor in lighting devices for industrial application.

2 Experimental

2. 1 Synthesis

A series of Eu^{3+} doped $CaMoO_4$ phosphors were synthesized through MSM. $CaCO_3$ (analytical reagent grade), MoO_3 (99.95%), and Eu_2O_3 (99.99%) were used as reaction precursors. Stoichiometric amounts of $CaCO_3$, MoO_3, and Eu_2O_3 were mixed together and then put into a household microwave oven. The microwave was turned on with its full output (800 W) for 35–60 min. For some cases, proper amounts of Li_2CO_3, Na_2CO_3, or K_2CO_3 were added as the charge compensators.

2. 2 Characterization

The structures were analyzed on an XD-2X/M4600 powder X-ray diffraction (XRD) with Cu Kα radiation with a voltage of 36 kV and an electric current of 30 mA (Beijing Purkinje General Instrument Corporation). The XRD patterns were recorded in the range of $15° < 2\theta < 70°$. The microstructure and morphology of the phosphors were observed by Quanta 400/INCA/HKL Thermal FE Environment scanning electron microscope (SEM). The excitation and emission spectra were recorded by an RF-5301 fluorescence spectrometer equipped with a xenon lamp as excitation source. The excitation slit and the emission slit were 3.0 nm and 3.0 nm, respectively. A centrifugal particle size analyzer LA-920 (HORIBA Instruments Inc.) was used to observe the distribution and size of the particles. All measurements were carried out at room temperature.

3 Results and discussion

3. 1 Powder XRD and structure

The XRD patterns of the typical Eu^{3+} doped $CaMoO_4$ phosphors without and with different charge compensators are shown in Fig. 1. All of them are in agreement with the standard JADE Card PDF#29-0351 and basically maintain characteristic of scheelite structure of space group $I4_1/a$ (No. 88) [17] with the cell parameters $a = b = 0.5223$ nm and $c = 1.142$ nm, implying that neither the doped Eu^{3+} ions nor charge compensators have apparent influence on the crystal structure.

The charge compensation mechanisms can be

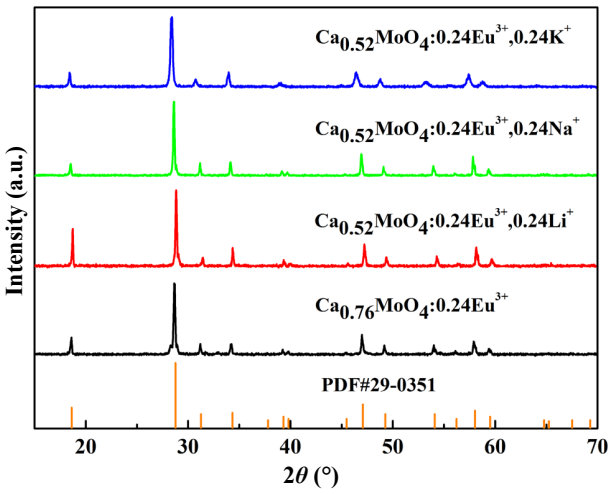

Fig. 1 XRD patterns of the typical $CaMoO_4:Eu^{3+}$ and $CaMoO_4:Eu^{3+},A^+$ (A = Li, Na, K) phosphors synthesized by MSM for 30 min.

explained as below. Two Ca^{2+} ions are replaced by one Eu^{3+} ion and one monovalent cation, $2Ca_{Ca}^{\times} \rightarrow Eu_{Ca}^{\cdot} + A'_{Ca}$, where A′ denotes a monovalent cation such as Li^+, Na^+, or K^+ which is acting as a charge compensator. It can be seen that the peak shifts to lower 2θ values as K^+ or Na^+ ions substitute Ca^{2+} ions, while the peak shifts to higher 2θ values as Li^+ ions substitute Ca^{2+} ions relatively [18]. These shifts should be attributed to the fact that the ionic radii of Na^+ (118 pm) and K^+ (138 pm) are larger than that of Ca^{2+} (112 pm), and the ionic radius of Li^+ (92 pm) [19] is smaller than that of Ca^{2+}. According to the Prague formula [20] $2d\sin\theta = n\lambda$ (d is the interplanar spacing, λ is the incident wavelength, θ is the angle between the incident light and the face of lattice), the smaller θ may be caused by the enlargement of interplanar spacing.

In Fig. 2(a), all diffraction peaks can be easily indexed to those of $CaMoO_4$ scheelite structure. The phases where the peaks appear are almost the same.

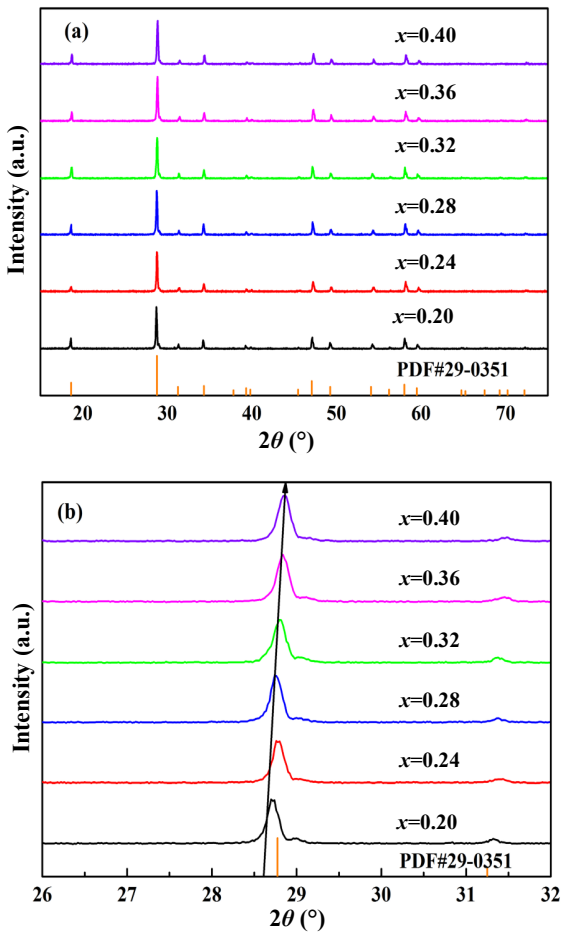

Fig. 2 (a) XRD patterns of the $Ca_{1-2x}MoO_4$:xEu^{3+},xLi^+ phosphors synthesized by MSM for 30 min. (b) Enlarged XRD patterns of the $Ca_{1-2x}MoO_4$:xEu^{3+},xLi^+ phosphors from 26° to 32°.

However, obvious deviations can be observed in the expanded version of the XRD spectra in Fig. 2(b) when compared with the exact positions of the peaks from the standard JADE Card PDF#29-0351. The deviations reflect a slight contraction of the unit cell due to the difference in ionic size of Ca^{2+} (112 pm), Li^+ (92 pm), and Eu^{3+} (107 pm) [21], which result in the distortion of scheelite structure.

The calcium molybdate crystal structure (Fig. 3) shows a high body-centered inversion symmetry [22]. This structure has eight symmetry elements, and a primitive cell includes two formula units of $CaMoO_4$. The Ca and Mo sites have S_4 point symmetry. Each Ca site is surrounded by eight O sites in approximately octahedral symmetry. Each Mo site is surrounded by four equivalent O sites to form $[MoO_4]^{2-}$ anions in approximately tetrahedral symmetry. Each O atom links with two Ca atoms and one Mo atom. There are two different Ca–O bond lengths in CaO_8 and one Mo–O bond length in $[MoO_4]^{2-}$. $CaMoO_4$ has strong covalent bonds of Mo–O in $[MoO_4]^{2-}$ molecular ionic units and weak coupling between $[MoO_4]^{2-}$ anions and Ca^{2+} cations [23–26].

3.2 Size distribution characterization

The morphology and size of phosphors are important for their applications in the encapsulation of lighting devices since their size and shape would affect the luminescence properties, heat dissipation efficiency, and reliability when the phosphors are coated onto InCaN chips [27]. Typical SEM images of $CaMoO_4$ samples prepared by MSM on full output (100%, 800 W) for 30 min are shown in Fig. 4(a) and Fig. 4(b) at different magnifications.

In Fig. 4(a), it can be seen that the phosphor powders are composed of slightly aggregated irregular

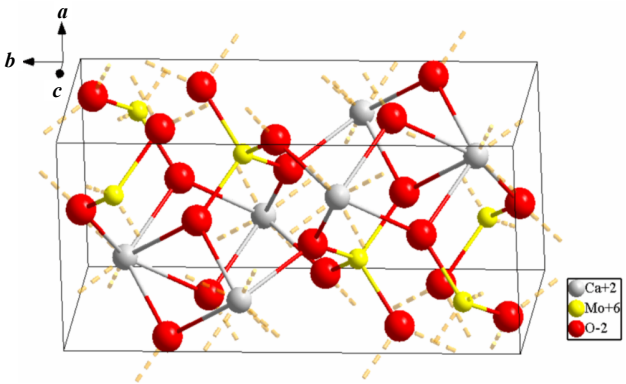

Fig. 3 Crystal structure of $CaMoO_4$.

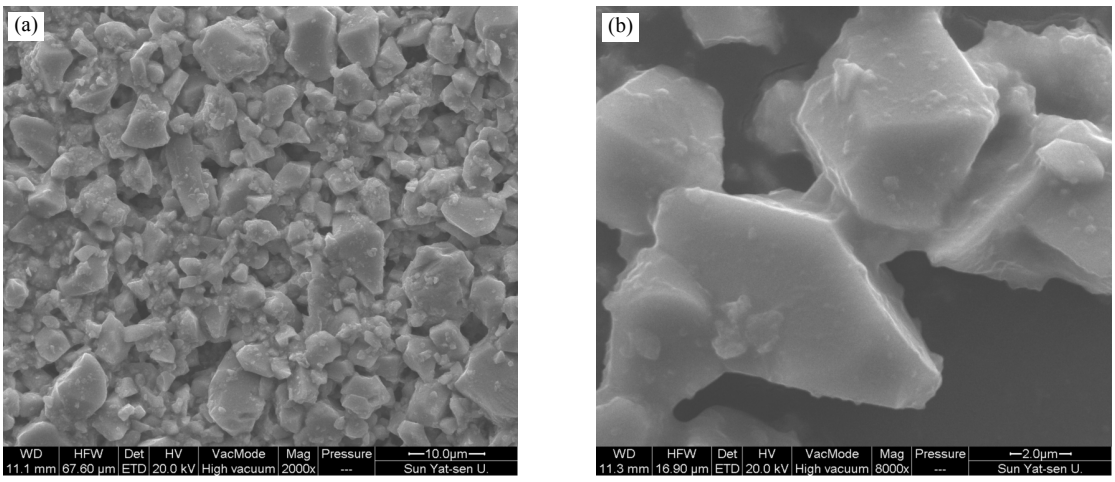

Fig. 4 SEM images of $CaMoO_4:Eu^{3+}$ phosphors synthesized by MSM for 30 min: (a) 2000× magnification, (b) 8000× magnification.

particles which are possibly due to quick heat molding by microwave radiation. The crystalline grains of the phosphors have a mean diameter of 2–8 μm. The enlarged SEM image in Fig. 4(b) shows that most of the particles are well dispersed octahedral shape which fits well the encapsulation requirement of white LEDs [27].

The particle size distribution shown in Fig. 5 is narrow, suggesting an average particle diameter of 3.82 μm, which is consistent with the SEM study. The particle size matches well with the phosphor size requirement for fluorescent lamp, indicating that the samples are promising for the fabrication of solid lighting devices.

3. 3 Luminescence properties

Figure 6 displays the excitation (λ_{ex} = 464 nm) and emission (λ_{em} = 615 nm) spectra of $Ca_{0.76}MoO_4$: $0.24Eu^{3+}$ and $Ca_{0.52}MoO_4$:$0.24Eu^{3+}$,$0.24A^+$ (A = Li, Na, K). The excitation and emission of all the samples are similar in both shape and position. The excitation

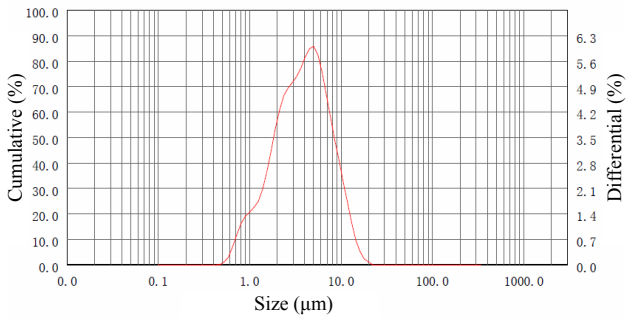

Fig. 5 Particle size distribution of $Ca_{0.36}MoO_4:0.32Eu^{3+}$, $0.32Li^+$ phosphor.

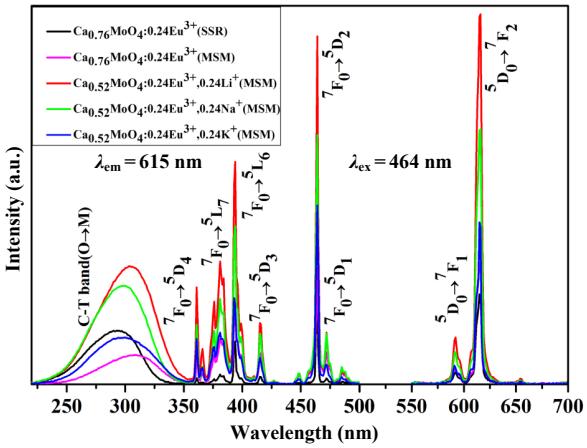

Fig. 6 Excitation and emission spectra of $Ca_{0.76}MoO_4$: $0.24Eu^{3+}$ and $Ca_{0.52}MoO_4$:$0.24Eu^{3+}$,$0.24A^+$ (A = Li, Na, K) synthesized by MSM for 30 min and $Ca_{0.76}MoO_4$: $0.24Eu^{3+}$ synthesized by SSR at 800 ℃ for 4 h.

spectra show that $CaMoO_4:Eu^{3+}$ has a broad charge transfer C–T band (O→Mo) in the UV region from 230 to 350 nm. The narrow peaks from 350 to 480 nm are the transitions from Eu^{3+} ground state to excited state of $4f^7$ configuration. The absorptions at 381 and 464 nm are due to the $^7F_0 \rightarrow {}^5L_6$ and $^7F_0 \rightarrow {}^5D_2$ transitions of Eu^{3+} ions, respectively. They are stronger than other peaks and match well with the emission wavelengths of near-UV or blue LED chips [28], and are expected to improve the color rendering property of commercial white LEDs.

Under 464 nm excitation, the emission spectra show the Eu^{3+} characteristic emissions, such as $^5D_0 \rightarrow {}^7F_1$ (593 nm) and $^5D_0 \rightarrow {}^7F_2$ (615 nm). As shown in Fig. 6, the relative intensity of $^5D_0 \rightarrow {}^7F_2$ is stronger than other peaks. The stronger red emission at 615 nm comes

from the electric dipole transition $^5D_0 \rightarrow {}^7F_2$, while the weak orange emission located at around 593 nm is due to the magnetic dipole transition $^5D_0 \rightarrow {}^7F_1$. According to the spin selection rule [28], if the Eu^{3+} ions occupy the host sites with inversion symmetry, optical transitions inside the 4f configuration are strictly forbidden as electric dipole transition, which means the electric dipole transition of $^5D_0 \rightarrow {}^7F_2$ is forbidden. However, when the 4f configuration of Eu^{3+} is mixed with the opposite configurations 5d and 5g, or the symmetry is deviated from the centre of inversion, the spin selection rule is relaxed and the forbidden transition of 4f energy levels is partially relieved, which may result in the electric dipole transition of $^5D_0 \rightarrow {}^7F_2$ and emit red light [29]. So it can be concluded that the Eu^{3+} ions are not located at the site with inversion symmetry for the phosphors.

The emission intensities of the phosphors synthesized by MSM with different charge compensators ($Ca_{0.52}MoO_4$:0.24Eu^{3+},0.24A^+(A = Li, Na, K)) are comparable and respectively about 4.5, 3, 1.5 times stronger than that of the phosphor without charge compensation. It reveals that lithium is the best charge compensator for $CaMoO_4$: Eu^{3+} because the ionic radius of Li^+ (92 pm) [19] is smaller than that of Ca^{2+}, which makes it more commodious to substitute Ca^{2+} ions. Besides, the red emission intensity of $Ca_{0.76}MoO_4$:0.24Eu^{3+} synthesized by MSM for 30 min is much stronger than that which is prepared by SSR at 800 ℃ for 4 h. Consequently, an enhanced red emission is observed in charge compensated phosphor samples, and MSM gets higher efficiency comparing with SSR.

Figure 7 shows the excitation and emission spectra of $Ca_{0.52}MoO_4$:0.24Eu^{3+},0.24Li^+ prepared by microwave sintering on full output (100%, 800 W) with the reaction time from 35 to 60 min. The emission intensity increases gradually as time increasing and then decreases beyond the reaction time of 55 min, as shown in the inset plot in Fig. 7. The $Ca_{0.52}MoO_4$: 0.24Eu^{3+},0.24Li^+ prepared at 55 min is found to have the highest emission. Compared with traditional high temperature solid phase method using 800 ℃ for 4 h [30] or co-precipitation method which precalcines samples at 500 ℃ for 2 h and then maintains at 800 ℃ for 4 h [31], MSM has significant advantages.

For maintaining the charge balance of $CaMoO_4$, equal concentrations of Eu^{3+} and Li^+ ions were used to compensate the charges of Ca^{2+}. Figure 8 shows that

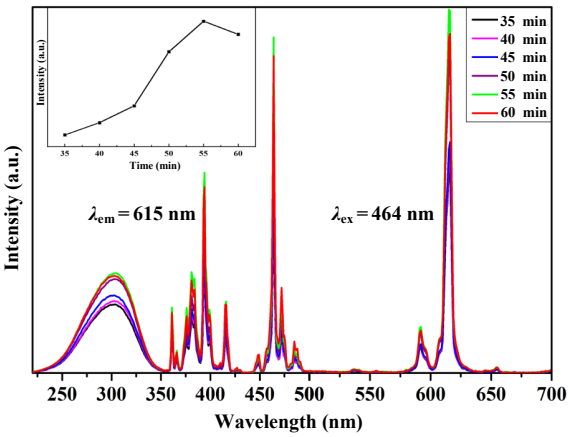

Fig. 7 Excitation and emission spectra of $Ca_{0.52}MoO_4$: 0.24Eu^{3+},0.24Li^+ synthesized by MSM at different sintering time. The inset shows the integrated emission intensity as a function of the reaction time.

the excitation and emission intensities of the $Ca_{1-2x}MoO_4$:$x$$Eu^{3+}$,$x$$Li^+$ have been strongly improved by the increasing Eu^{3+} and Li^+ dopant concentration. In addition, the ionic radius of Li^+ (92 pm) is smaller than that of Ca^{2+}, which guarantees the substitution of Ca^{2+} ions and the entrance to lattice matrix without changing the shape and positions of spectrum peaks. However, this leads to the lattice distortion and symmetry reduction that improve the probability of the electric dipole transition $^5D_0 \rightarrow {}^7F_2$. Thus, effective enhancement appears at red emission peak of 615 nm. In general, the photoluminescence intensity increases with the concentration of the activators in its low concentration range but decreases in high concentration range due to concentration quenching [32]. As it is observed in Fig. 8, the intensities of all emissions are enhanced significantly as the Eu^{3+} concentration increases before it reaches 32 mol%. Thus concentration quenching occurs after this point, so this is the optimized Eu^{3+} concentration for maximum emission intensity for $Ca_{1-2x}MoO_4$:$x$$Eu^{3+}$, $x$$Li^+$.

As shown in the inset of Fig. 8, the red emission intensity of $Ca_{0.36}MoO_4$:0.32Eu^{3+},0.32Li^+ synthesized by MSM for 30 min is no less than that which synthesized by SSR at 800 ℃ for 4 h. Furthermore, the samples synthesized by MSM are much more loose and very easy to handle, while that which synthesized by SSR are too hard and difficult to grind. In addition, the optimized sample $Ca_{0.36}MoO_4$:0.32Eu^{3+},0.32Li^+ synthesized by MSM has an enhancement factor of 4 in photoluminescence in comparison with the sample made without charge compensation compounded

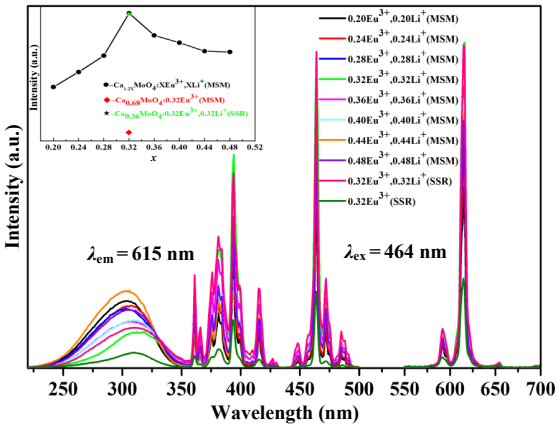

Fig. 8 Excitation and emission spectra of $Ca_{1-2x}MoO_4$:xEu^{3+},xLi^+ (x = 0.20–0.48) synthesized by MSM for 30 min and synthesized by SSR at 800 ℃ for 4 h. The inset shows the integrated emission intensity as a function of the concentration of Eu^{3+} and Li^+.

in the same way. All of these certify that charge compensator can lead to the luminescence enhancement and $CaMoO_4$:Eu^{3+},Li^+ can be heated internally and externally at the same time quickly and evenly with strong intensity, which is more time-saving as well as energy-saving than SSR. This indicates that the MSM should be considered competent for other metal molybdates or tungstates preparation.

Moreover, as the Eu^{3+} concentration increases, the maxima of broad charge transfer bands shifts from 292 to 310 nm (Fig. 8). As a general rule, the energy level that is influenced by the configuration of $CaMoO_4$ changes between the ground state and the excited state or the first excited state and the ground state, which makes a difference in photon absorption or emission. Therefore, the wavelengths shift to right as shown in the photoluminescence excitation (PLE) spectra [33].

3. 4 Chromaticity of $CaMoO_4$:Eu^{3+},A^+ phosphor

The Commission Internationale de l´Eclairage (CIE) chromaticity coordinates of a phosphor play an important qualification sign for luminescence applications. Figure 9 and Table 1 provide a summary (in graphic and tabular forms, respectively) of the CIE chromaticity of a single-phased emission-tunable phosphor. The CIE chromaticity coordinates are calculated by CIE calculate software with the result of x = 0.661 and y = 0.339 for the $Ca_{0.36}MoO_4$:$0.32Eu^{3+}$, $0.32Li^+$ phosphor synthesized by MSM for 30 min. The obtained coordinates are very close to National Television Standard Committee (NTSC) CIE

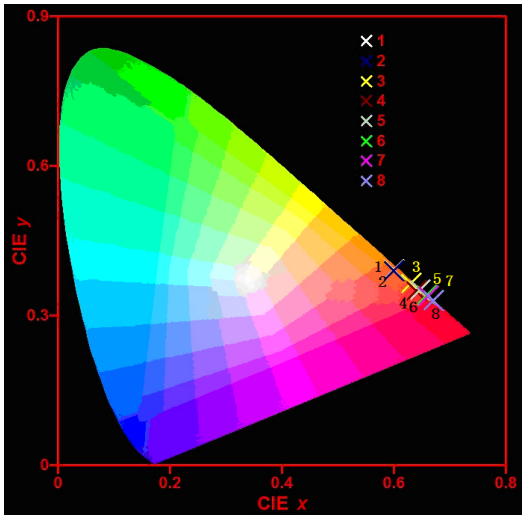

Fig. 9 CIE (1931) chromatic coordinates of $CaMoO_4$:Eu^{3+},A^+ phosphors. Numbers shown in the figure correspond to those described in Table 1.

Table 1 CIE chromatic coordinates of $CaMoO_4$:Eu^{3+} phosphors excited at 464 nm

No.	Composition	CIE (x, y)
1	$Ca_{0.76}MoO_4$:$0.24Eu^{3+}$ (SSR)	(0.600, 0.392)
2	$Ca_{0.76}MoO_4$:$0.24Eu^{3+}$ (MSM)	(0.602, 0.389)
3	$Ca_{0.52}MoO_4$:$0.24Eu^{3+}$,$0.24K^+$ (MSM)	(0.631, 0.364)
4	$Ca_{0.52}MoO_4$:$0.24Eu^{3+}$,$0.24Na^+$ (MSM)	(0.644, 0.353)
5	$Ca_{0.52}MoO_4$:$0.24Eu^{3+}$,$0.24Li^+$ (MSM)	(0.647, 0.351)
6	$Ca_{0.36}MoO_4$:$0.32Eu^{3+}$,$0.32Li^+$ (SSR)	(0.659, 0.340)
7	$Ca_{0.36}MoO_4$:$0.32Eu^{3+}$,$0.32Li^+$ (MSM)	(0.661, 0.339)
8	NTSC standard red	(0.670, 0.330)

values for red (x = 0.670, y = 0.330). Therefore, the $Ca_{0.36}MoO_4$:$0.32Eu^{3+}$,$0.32Li^+$ red phosphor would be a promising candidate for future white LED fabrication.

4 Conclusions

In summary, $CaMoO_4$:Eu^{3+} and $CaMoO_4$:Eu^{3+},A^+ (A = Li, Na, K) phosphors have been synthesized by microwave sintering method, which exhibit red luminescence with the strongest emission and excitation peaks at 615 nm and 464 nm, respectively. The SEM images have shown that the crystalline grains of the phosphors have a mean diameter of 2–8 μm, fitting well with the encapsulation requirement of white LEDs. The samples synthesized by MSM for 55 min were found to have the highest emission. The introduction of charge compensators (Li^+, Na^+, K^+) can enhance the luminescence enhancement of $CaMoO_4$:Eu^{3+}. The $Ca_{0.36}MoO_4$:$0.32Eu^{3+}$,$0.32Li^+$ phosphor, with the average particle diameter of 3.82 μm, shows the best red emission. All the results indicate that the

$Ca_{0.36}MoO_4$:0.32Eu^{3+},0.32Li^+ phosphor would be very promising in the applications of white lighting.

Acknowledgements

This work is supported by the National Natural Science Foundation of China (No. 21271074), teamwork projects funded by Guangdong Natural Science Foundation (No. S2013030012842), and CAS-Foshan Cooperation Funding Program (No. 2012HY100685).

References

[1] Nakamura S, Fasol G. *The Blue Laser Diode*, *GaN Based Light Emitters and Lasers*. New York: Springer Berlin Heidelberg, 1997: 216.

[2] Zhang X, Gong M. A new red-emitting Ce^{3+}, Mn^{2+}-doped barium lithium silicate phosphor for NUV LED application. *Mater Lett* 2011, **65**: 1756–1758.

[3] Guo C, Li M, Xu Y, *et al*. A potential green-emitting phosphor $Ca_8Mg(SiO_4)_4Cl_2$:Eu^{2+} for white light emitting diodes prepared by sol–gel method. *Appl Surf Sci* 2011, **257**: 8836–8839.

[4] Qiu Z, Zhou Y, Lü M, *et al*. Combustion synthesis of long-persistent luminescent MAl_2O_4:Eu^{2+}, R^{3+} (M = Sr, Ba, Ca, R = Dy, Nd and La) nanoparticles and luminescence mechanism research. *Acta Mater* 2007, **55**: 2615–2620.

[5] Kuznik W, Brik MG, Cieślik I, *et al*. Changes of fluorescent spectral features after successive rare earth doping of gadolinium oxide powders. *J Alloys Compd* 2012, **511**: 221–225.

[6] Kumar GA, Pokhrel M, Martinez A, *et al*. Synthesis and spectroscopy of color tunable Y_2O_2S:Yb^{3+}, Er^{3+} phosphors with intense emission. *J Alloys Compd* 2012, **513**: 559–565.

[7] Chung JH, Ryu JH, Eun JW, *et al*. Green upconversion luminescence from poly-crystalline Yb^{3+}, Er^{3+} co-doped $CaMoO_4$. *J Alloys Compd* 2012, **522**: 30–34.

[8] Xie R-J, Mitomo M, Uheda K, *et al*. Preparation and luminescence spectra of calcium- and rare-earth (R = Eu, Tb, and Pr)-codoped α-SiAlON ceramics. *J Am Ceram Soc* 2002, **85**: 1229–1234.

[9] Yen WM, Shionoya S, Yamamoto H. *Phosphor Handbook*, 2nd edn. Boca Raton: CRC Press, 2007: 533.

[10] Wang Z, Liang H, Gong M, *et al*. A potential red-emitting phosphor for LED solid-state lighting. *Electrochem Solid-State Lett* 2005, **8**: H33–H35.

[11] Neeraj S, Kijima N, Cheetham AK. Novel red phosphors for solid-state lighting: The system $NaM(WO_4)_{2-x}(MoO_4)_x$:Eu^{3+} (M = Gd, Y, Bi). *Chem Phys Lett* 2004, **387**: 2–6.

[12] Kim T, Kang S. Potential red phosphor for UV-white LED device. *J Lumin* 2007, **122–123**: 964–966.

[13] Tian L, Yang P, Wu H, *et al*. Luminescence properties of Y_2WO_6:Eu^{3+} incorporated with Mo^{6+} or Bi^{3+} ions as red phosphors for light-emitting diode applications. *J Lumin* 2010, **130**: 717–721.

[14] Ekambaram S, Maaza M. Combustion synthesis and luminescent properties of Eu^{3+}-activated cheap red phosphors. *J Alloys Compd* 2005, **395**: 132–134.

[15] Li YQ, van Steen JEJ, van Krevel JWH, *et al*. Luminescence properties of red-emitting $M_2Si_5N_8$:Eu^{2+} (M = Ca, Sr, Ba) LED conversion phosphors. *J Alloys Compd* 2006, **417**: 273–279.

[16] Hu Y, Zhuang W, Ye H, *et al*. A novel red phosphor for white light emitting diodes. *J Alloys Compd* 2005, **390**: 226–229.

[17] Teshima K, Yubuta K, Sugiura S, *et al*. Selective growth of calcium molybdate whiskers by rapid cooling of a sodium chloride flux. *Cryst Growth Des* 2006, **6**: 1598–1601.

[18] Liu J, Lian H, Shi C. Improved optical photoluminescence by charge compensation in the phosphor system $CaMoO_4$:Eu^{3+}. *Opt Mater* 2007, **29**: 1591–1594.

[19] Lin YS, Liu RS, Cheng B-M. Investigation of the luminescent properties of Tb^{3+}-substituted YAG:Ce, Gd phosphors. *J Elechem Soc* 2005, **152**: J41–J45.

[20] De Vries JL. The early years of X-ray diffraction and X-ray spectrometry. In: *Advances in X-ray Analysis*, *Vol. 39*. Gilfrich JV, *et al*. Eds. New York: Plenum Press, 1997: 1–11.

[21] Shannon RD, Prewitt CT. Effective ionic radii in oxides and fluorides. *Acta Cryst* 1969, **B25**: 925–946.

[22] Achary SN, Patwe SJ, Mathews MD, *et al*. High temperature crystal chemistry and thermal expansion of synthetic powellite ($CaMoO_4$): A high temperature X-ray diffraction (HT-XRD) study. *J Phys Chem Solids* 2006, **67**: 774–781.

[23] Liu H, Tan L. Synthesis, structure, and electrochemical properties of $CdMoO_4$ nanorods. *Ionics* 2010, **16**: 57–60.

[24] Phuruangrat A, Thongtem T, Thongtem S. Synthesis of lead molybdate and lead tungstate via microwave irradiation method. *J Cryst Growth* 2009, **311**: 4076–4081.

[25] Fujita M, Itoh M, Katagiri T, *et al*. Optical anisotropy and electronic structures of $CdMoO_4$ and $CdWO_4$ crystals: Polarized reflection measurements, X-ray photoelectron spectroscopy, and electronic structure calculations. *Phy Rev B* 2008, **77**: 155118.

[26] Abraham Y, Holzwarth NAW, Williams RT. Electronic structure and optical properties of $CdMoO_4$ and $CdWO_4$. *Phy Rev B* 2000, **62**: 1733.

[27] Liu J, Kang M, Sun R, *et al*. Study on luminescent properties of red phosphor CaO:Eu^{3+} prepared by co-precipitation method. *New Chemical Materials* 2009, **37**: 23–25. (in Chinese)

[28] Zhang Z-J, Chen H-H, Yang X-X, *et al*. Preparation and luminescent properties of Eu^{3+} and Tb^{3+} ions in the host of $CaMoO_4$. *Mater Sci Eng B* 2007, **145**: 34–40.

[29] Yan B, Wu J-H. $NaY(MoO_4)_2:Eu^{3+}$ and $NaY_{0.9}Bi_{0.1}(MoO_4)_2:Eu^{3+}$ submicrometer phosphors: Hydrothermal synthesis assisted by room temperature-solid state reaction, microstructure and photoluminescence. *Mater Chem Phys* 2009, **116**: 67–71.

[30] Zhang F, Lv S. Preparation and luminescence properties of $CaMoO_4:Eu^{3+}$ phopher. *Natural Science Journal of Harbin Normal University* 2010, **26**: 45–48. (in Chinese)

[31] Yang Y, Li X, Feng W, *et al*. Effect of surfactants on morphology and luminescent properties of $CaMoO_4:Eu^{3+}$ red phosphors. *J Alloys Compd* 2011, **509**: 845–848.

[32] Mao Y, Ding F, Gu Y. The influence of concentration of Yb^{3+} ions on luminescence and fluorescence lifetime in Yb:YAG crystals. *Acta Photonica Sinica* 2006, **35**: 365–368. (in Chinese)

[33] Li B, Li J, Zhao J. Fine-tuning the fluorescence emission wavelength of gold nanoclusters in the protein-directed synthesis: The effect of silver ions. *J Nanosci Nanotechno* 2012, **12**: 8879–8885.